Numerical algorithm for modelling multicomponent multipermeator systems

A. Makaruk, M. Harasek*

Vienna University of Technology, Institute of Chemical Engineering, Getreidemarkt 9/166, 1060 Vienna, Austria

ARTICLE INFO

ABSTRACT

The presented algorithm allows calculation of multicomponent gas separation in hollow-fibre membrane modules in co-current, counter-current and cross-flow configurations. The permeators can be combined in any system with recycles. The algorithm is based on the finite difference Gauß–Seidel method. The solution of the system can be stabilised by means of adaptation of the relaxation factor in case of difficulties with convergence. The performance of the algorithm was evaluated in terms of the required number of iterations and computational time for a number of single permeator and multipermeator separation problems. The counter-current configuration with component gases having high selectivities required the most computational time.

The permeation of a biogas-like gas mixture consisting of three components: methane, carbon dioxide and oxygen was modelled and compared with an experiment. The results of the modelled gas separation were found to be in good agreement with the measured values. The highest performance was achieved by the counter-current configuration.

© 2009 Elsevier B.V. All rights reserved.

1. Introduction

The mathematical modelling is an indispensable tool in the design of gas permeation systems. The interest for the modelling of membrane permeators appeared already with their first implementations. One of the first mathematical formulations of the flow in gas permeators can be attributed to Stern and Wang [1]. The authors defined material balances using ordinary differential equations for binary mixtures in a single permeator and tried to solve them using the trial-and-error method. Similar methods were used in further studies [2,3] and proved to converge with difficulties especially if an inadequate initial guess was given.

Pan [4] formulated governing equations for multicomponent permeation systems assuming that all considered flow configurations can be approximated as the cross-flow configuration. The equations could be solved using the trial-and-error method or an iterative method. For the iterative method, the concentration of one component in the residue had to be provided. A similar method was used by Bhide and Stern [5,6] to identify the optimal process configurations for the natural gas treatment and for the production of oxygen from air. Probably the greatest disadvantage of Pan's formulation is the simplification of the flow on the permeate side. As a result, the model does not predict the permeation correctly for

higher stage cuts [4]. Kaldis et al. [7] suggested that Pan's equations could be solved using the orthogonal collocation method. However, they assumed a constant concentration profile on the permeate side. The algorithm delivered only approximate solutions and the computational effort increased greatly if higher accuracy was required. More recently, Chowdhury et al. [8] proposed a new numerical algorithm for the Pan's equations and implemented the solver into a commercial process simulation tool.

The Runge–Kutta integrators represent a set of successful numerical techniques for the modelling of gas permeators [9–11]. However, the methods benefit from the fact that the problem of permeation of binary mixtures can be reduced to a single differential equation. As a result only permeation of binary mixtures can be approached with these methods. Moreover, the implementation of the integrators can be cumbersome if used in the modelling of multistage systems.

Thundyil and Koros [12] presented a method for the modelling of three configurations: co-current, counter-current and, as first, radial cross-flow. In the model named 'succession of states', the mass balances were calculated with an iterative method for a finite number of states/elements. Although the model could be extended to cope with multicomponent systems, solely equations for binary systems were presented.

Coker et al. [13] transformed conservation equations for a single permeator into the form that could be fitted into a tridiagonal matrix. Subsequently, the matrix was solved using the Thomas algorithm. The feed and permeate flows were modelled in detail. However, it was not revealed how the method could handle the modelling of multistage systems with recycles.

* Corresponding author. Tel.: +43 1 58801 15925; fax: +43 1 58801 15999.
  E-mail addresses: aleksander.makaruk@tuwien.ac.at (A. Makaruk),
michael.harasek@tuwien.ac.at (M. Harasek).
  URL: http://www.thvt.at/ (M. Harasek).

Also, averaging methods are applied successfully in the modelling of gas permeation. Chen et al. [14] presented a method based upon the concept of the average driving force approximation. The results provided by the approximate model were in very good agreement with the exact solutions for lower stage cuts. Furthermore, the model could calculate cases with a high number of components achieving at the same time reasonable computational times. A similar approach was used in the work of Pettersen and Lien [15], where the analogy to heat exchanger systems and the concept of the logarithmic mean of driving force were applied.

Some part of the most recent research on gas permeation systems focuses on optimisation algorithms [16–19]. Optimisation tools require robust gas permeation models in order to predict the behaviour of a permeator system correctly. However, it can be noticed that the contemporary optimisation tools use simplified gas permeation models, which could suggest that the algorithms for detailed gas permeation models are not reliable enough to be used together with advanced optimisation algorithms.

In this work, a numerical method is presented that is able to model multicomponent multistage hollow-fibre membrane systems. The algorithm is an iterative approach based on the finite difference Gauß–Seidel method and can calculate the permeation in co-current, cross-flow and counter-current flow configurations. The algorithm is easy to program, effective and can cope with additional nonlinearities like variable permeances or pressure loss. The performance of the solver, i.e. computational effort and convergence, is evaluated for a few single stage and multistage permeation problems. The results obtained from the modelling are verified experimentally for a biogas-like gas mixture consisting of methane, carbon dioxide and oxygen.

2. Modelling

2.1. Governing equations

The starting point is the definition of the conservation of component gases in one dimension for the feed channel and for the permeate channel. In this work, the Standard Temperature and Pressure (STP) volume is used to account for the amount of gas. The conservation of each component is considered separately. Under the assumption that the partial volume flow of a gas component i changes due to its local trans-membrane flow, the conservation equations can be expressed by

$$\frac{dF_i}{dl} = -Q_i', \tag{1}$$

$$\frac{dP_i}{dl} = Q_i', \tag{2}$$

where F and P are volume flows in the feed channel and in the permeate channel respectively, l is the longitudinal coordinate of the membrane and Q is the local trans-membrane flow. In hollow-fibre gas permeators, the local trans-membrane flow is usually modelled using the solution-diffusion equation [20]:

$$Q_i' = Q_i'' s\pi d = \Pi_i(x_i p_F - y_i p_P)s\pi d, \tag{3}$$

where s is the total number of fibres, d is the diameter of the active layer, Π is the permeance, p is the absolute pressure and x and y are the volume fractions in the feed channel and in the permeate channel respectively. Since perfect gas is assumed, volume fractions are equal to molar fractions.

The permeance depends on a series of process parameters like temperature, pressure or the flux coupling with other gas components and can be included in the presented model if the required relations are known:

$$\Pi_i = f(T, p_F, p_P, x_0, x_1, \ldots, y_0, y_1, \ldots). \tag{4}$$

The conservation equations for a component i given by Eqs. (1) and (2) are coupled with the conservation equations of other gas components by means of the following expressions:

$$x_i = \frac{F_i}{\sum_{i=1}^{k} F_i}, \tag{5}$$

$$y_i = \frac{P_i}{\sum_{i=1}^{k} P_i}. \tag{6}$$

In the cross-flow configuration there is no permeate flow along the membrane and the concentration in the permeate channel is given by

$$y_i = \frac{Q_i}{\sum_{i=1}^{k} Q_i}. \tag{7}$$

The system to be solved consists of $2k$ coupled nonlinear differential equations, where k is the number of gas components. The system can consist of additional equations that influence the result of the modelling by varying process parameters. For example, if the high pressure feed is on the bore-side, the pressure loss generated in the laminar flow along the distance Δl can be expressed by

$$\Delta p_F = \frac{\sum_{i=1}^{k} F_i \eta 128 \,\Delta l p_{STP} T_F}{s\pi D^4 p_F T_{STP}}, \tag{8}$$

where η is the dynamic viscosity of the gas and D is the internal diameter of the fibre. The above equation represents the Hagen–Poiseuille law in the form suitable for systems that use STP volume flows. The dynamic viscosity η that influences the pressure loss and, as a result, the permeation of the component gases also depends on the concentration of component gases. This introduces an additional coupling factor that the numerical method must cope with.

2.2. Numerical algorithm

Eqs. (1) and (2) can be interpreted as one-dimensional Poisson equations, which are elliptic partial differential equations. The solution of elliptic partial differential equations can be attempted by various methods, for which numerous references are available in literature. The method suggested in this work derives from the iterative finite difference Gauß–Seidel method [21]. The finite difference discretisations for three flow configurations: co-current, cross-flow and counter-current for a single component i and in a domain consisting of c discrete points are presented in Fig. 1. The points with the index $j = 1$ are used for the specification of boundary conditions of Dirichlet type [21] and do not participate in the trans-membrane flow.

The volume flow gradients are approximated using the first order upwind finite difference scheme:

$$\frac{dF_{i,j}}{dl} = \frac{F_{i,j} - F_{i,j-1}}{\Delta l}, \tag{9}$$

$$\frac{dP_{i,j}}{dl} = \frac{P_{i,j} - P_{i,j-1}}{\Delta l}. \tag{10}$$

Hence Eqs. (1) and (2) can be transformed to calculate the value of STP volume flows for a specific gas component i at a discrete

COCURRENT
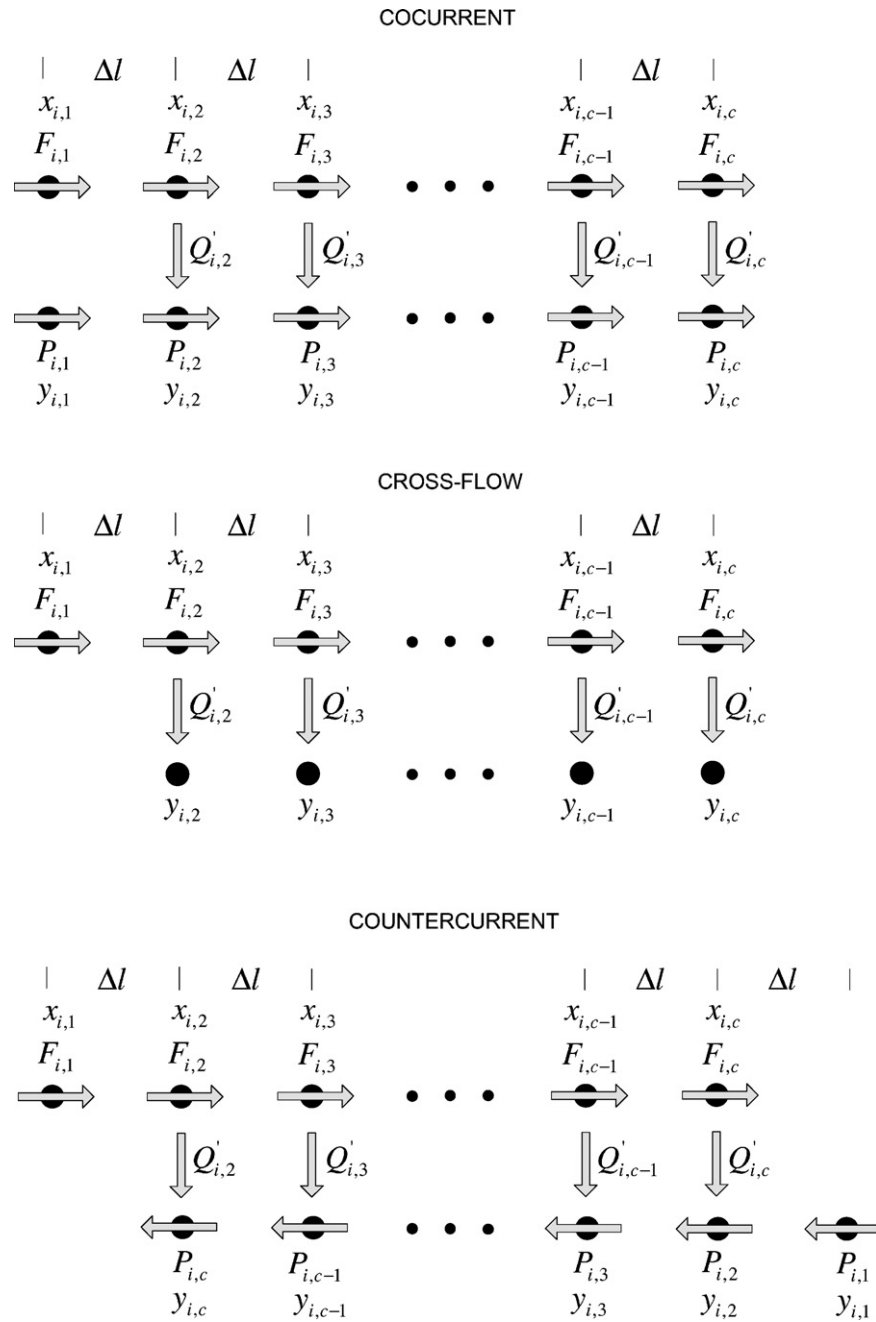

CROSS-FLOW

COUNTERCURRENT

Fig. 1. 1D finite difference discretisations for co-current, cross-flow and counter-current flow configurations.

point j. The corresponding equations for the co-current configuration are:

$$F_{i,j}^{n+(1/2)} = F_{i,j-1}^n - \Delta l \Pi_{i,j}^n (x_{i,j}^n p_{F,j}^n - y_{i,j}^n p_{P,j}^n) s\pi d \qquad (11)$$

$$P_{i,j}^{n+(1/2)} = P_{i,j-1}^n + \Delta l \Pi_{i,j}^n (x_{i,j}^n p_{F,j}^n - y_{i,j}^n p_{P,j}^n) s\pi d \qquad (12)$$

In the permeate channel of the cross-flow configuration there is no permeate flow along the membrane, therefore the volume conservation in the permeate channel is expressed simply by

$$Q_{i,j}^{n+(1/2)} = \Delta l \Pi_{i,j}^n (x_{i,j}^n p_{F,j}^n - y_{i,j}^n p_{P,j}^n) s\pi d \qquad (13)$$

As for the counter-current flow configuration the equations are:

$$F_{i,j}^{n+(1/2)} = F_{i,j-1}^n - \Delta l \Pi_{i,j}^n (x_{i,j}^n p_{F,j}^n - y_{i,c-j+2}^n p_{P,c-j+2}^n) s\pi d \qquad (14)$$

$$P_{i,j}^{n+(1/2)} = P_{i,j-1}^n + \Delta l \Pi_{i,j}^n (x_{i,c-j+2}^n p_{F,c-j+2}^n - y_{i,j}^n p_{P,j}^n) s\pi d \qquad (15)$$

A new variable n has been introduced in the aforementioned equations. The variable n denotes the state of the variables before the iteration step, $n + (1/2)$ denotes the half-step variables and $n + 1$ denotes the variables after the iteration is completed. The full iteration step for the feed channel and for the permeate channel is expressed by the following extrapolations:

$$F_{i,j}^{n+1} = F_{i,j}^n + \varpi(F_{i,j}^{n+(1/2)} - F_{i,j}^n), \qquad (16)$$

$$P_{i,j}^{n+1} = P_{i,j}^n + \varpi(P_{i,j}^{n+(1/2)} - P_{i,j}^n), \qquad (17)$$

and in the permeate channel for the cross-flow configuration by

$$Q_{i,j}^{n+1} = Q_{i,j}^n + \varpi(Q_{i,j}^{n+(1/2)} - Q_{i,j}^n), \tag{18}$$

where ϖ is the relaxation factor.

The solution procedure is relatively straightforward. The solver loops over the discrete points performing the half-step and full-step operations for each discrete point. The flow variables are updated instantly so that they can be used in the calculations of the next point. The looping is performed always in the direction of the flow as visualised in Fig. 1. The feed flow is calculated from left to right regardless of the configuration used. The permeate flow in the co-current configuration is calculated from left to right. In the counter-current configuration, the permeate flow is calculated from right to left. The permeate flow in the cross-flow configuration can be calculated in both directions. After the extrapolation of volume flows for each discrete point has been completed, the concentrations are calculated for the next iteration step using Eqs. (5) and (6) or (7). At this point, other dependent variables like pressure or variable permeability are calculated as well. For instance the pressure profile in the feed channel can be obtained from

$$p_{F,j} = p_{F,j-1} - \frac{\sum_{i=1}^{k} F_{i,j}\eta_j 128 \Delta l p_{STP} T_{F,j-1}}{s\pi D^4 T_{STP} p_{F,j-1}}. \tag{19}$$

If an exact calculation of pressure loss is required, the dynamic viscosity can be calculated at discrete points from the gas concentrations using the methods of Chung and Wilke, which were described in detail in [22].

The solver proceeds with the iterations until the convergence criterion for every gas component and every discrete point is met

$$|F_{i,j}^{n+(1/2)} - F_{i,j}^n| \leq \delta, \tag{20}$$

where δ is the convergence criterion. In the aforementioned equation, the partial feed volume flow at the beginning of an iteration step is subtracted from the partial feed volume flow calculated at the half-step. If for every discrete point the absolute value of this difference is smaller than or equal to δ, the solution is assumed to be convergent. The value of δ should be chosen with caution; excessively high values will lead to false results, excessively low values will result in a very high iteration number. Typically, we choose δ to be at least one thousandth of the smallest component volume flow in the model, i.e. if the smallest feed volume flow of a gas component were $1 \, m^3/s$, a reasonable value for δ could be $0.001 \, m^3/s$.

The first iteration step in the solution procedure requires some initial values of the gas concentrations for both feed and permeate side of the membrane. These can be given for each of the discrete points by rough initial guesses:

$$x_{i,j} = x_{i,1} \tag{21}$$

$$y_{i,j} = \frac{x_{i,j}\Pi_i}{\sum_{i=1}^{k} x_{i,j}\Pi_i} \tag{22}$$

If the calculation of pressure loss is required, the initial values for pressures must be provided for each of the discrete points. For the initial values it is enough to distribute the feed and permeate pressure along the membrane:

$$p_{F,j} = p_{F,1} \tag{23}$$

$$p_{P,j} = p_{P,1} \tag{24}$$

The solution procedure is visualised in Fig. 2. A more detailed description of the algorithm for a multistage case can be found in Appendix A.
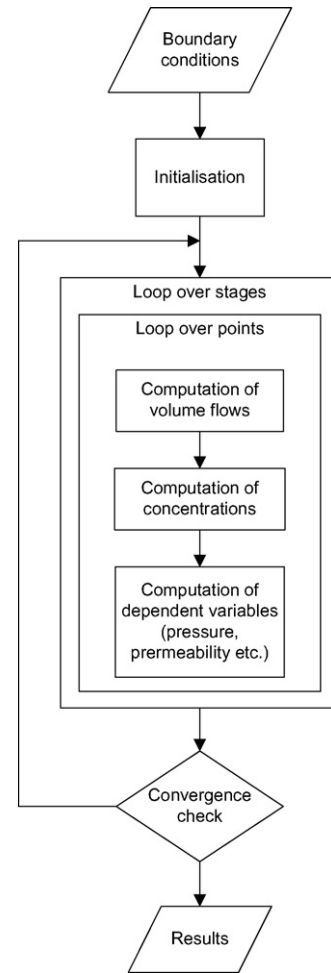

Fig. 2. Solution procedure.

2.3. Model evaluation – simplifications

The equations presented in the previous sections provide a simplified interpretation of the flow in gas permeators and certain assumptions have been made. Firstly, it is assumed that the flow in the permeator is perfectly one-dimensional. Secondly, it is assumed that there is no diffusion or dispersion of gas components in the direction parallel to the membrane. Furthermore, we neglect the concentration polarisation normal to the membrane. A few theoretical [23–25] and experimental studies [26] were performed on the topic of concentration polarisation in gas permeation. Mourgues and Sanchez [23] report in their theoretical investigation that there exist certain values of selectivity and permeance above which the phenomenon of concentration polarisation in hollow fibres becomes significant. Typically, concentration polarisation needs to be taken into account for membranes with high permeances and for separations of gas–vapour mixtures [26]. For example, the stagnant film theory combined with mass transfer coefficients [27] could be used to model concentration polarisation effects for each of the discrete points in the presented model. In this case, a high-selective system should be investigated experimentally to verify the results provided by the model.

Typically, the behaviour of gas permeation in real processes diverges from the simple solution-diffusion equation. In isothermal conditions, the permeance of a single gas can be influenced by pressure effects [28,29] and by the polymer swelling induced by the permeation of carbon dioxide [29]. The present algorithm is able to calculate permeation processes where the permeance is

Table 1
Computational effort for several permeator configurations.

Gas components	System	Discrete points	ϖ	δ (m³/s)	Iterations	CPU time (s)
$x_{CH_4} = 0.65, x_{CO_2} = 0.35$	Single co-current	200	0.9	1e−5	23	0.27
$x_{CH_4} = 0.65, x_{CO_2} = 0.35$	Single counter-current	200	0.4	1e−5	561	5.17
$x_{CH_4} = 0.65, x_{CO_2} = 0.34, x_{O_2} = 0.01$	Single counter-current	200	0.4	1e−6	370	4.86
$x_{CH_4} = 0.65, x_{CO_2} = 0.335, x_{O_2} = 0.01, x_{H_2O} = 0.005$	Single co-current	200	0.7	1e−6	70	1.15
$x_{CH_4} = 0.65, x_{CO_2} = 0.335, x_{O_2} = 0.01, x_{H_2O} = 0.005$	Single counter-current	200	0.05	1e−6	6,044	90.92
$x_{CH_4} = 0.65, x_{CO_2} = 0.335, x_{O_2} = 0.01, x_{H_2O} = 0.005$	Two counter-current stages LP1-2b [30]	200	0.05	1e−6	6,280	96.59
$x_{CH_4} = 0.65, x_{CO_2} = 0.335, x_{O_2} = 0.01, x_{H_2O} = 0.005$	Two counter-current stages LP1-2b [30]	400	0.05	1e−6	10,350	321.56
$x_{CH_4} = 0.65, x_{CO_2} = 0.34, x_{O_2} = 0.01$	Two counter-current stages LP1-2b [30]	400	0.4	1e−6	1,272	32.58
$x_{CH_4} = 0.65, x_{CO_2} = 0.34, x_{O_2} = 0.01$	Three counter-current stages LP1-3a [30]	400	0.4	1e−6	381	49.82

a function of other process parameters. However, we use constant permeances and the solution-diffusion model in its basic form in the modelling examples given in this work.

2.4. Model evaluation – numerical robustness

In the present algorithm, the proper choice of both solver parameters: relaxation factor ϖ and convergence criterion δ is vital for the successful solution of the equations. Basically, the system of equations requires to be under-relaxed, i.e. ϖ needs to be smaller than 1. Higher ϖ values generally result in lower computational times. However, difficult systems like stiff systems or systems with variable permeances require the reduction of ϖ values and higher numbers of iterations to approach a convergent solution. For simple systems with few components and moderate selectivities, the relaxation factors are typically between 0.4 and 0.9. For systems with high stiffness caused by high selectivities, the fast permeating components can make the solution unstable. For such problems, the reduction of the relaxation factor down to 0.05 is necessary to obtain a convergent solution.

In literature, the computational effort for the complete solution of nonlinear differential equations in multicomponent permeator systems is frequently considered to be much higher than for approximate solutions [7,14,15,17]. Therefore it is necessary to evaluate the computational efficiency of a new algorithm that deals with the detailed modelling of gas permeation, so that it can be used as a reference point for other computational methods.

Table 1 presents results of the computational effort that is required for the solution of a number of permeator systems. The computational tests were performed on a machine using 2.2 GHz AMD-Athlon 64™ processor. The solver was programmed in Matlab® 7. The ideal selectivities of the membrane were: $\alpha_{CO_2/CH_4} = 40$, $\alpha_{O_2/CH_4} = 6.66$ and $\alpha_{H_2O/CH_4} = 200$. The feed volume flow equaled $1\,m^3_{STP}/s$. The calculation of pressure loss using the variable dynamic viscosity was included in the model.

It can be seen that for simple single unit systems, convergence is reached within seconds. Generally, the counter-current configuration needs lower relaxation factors and is much more computationally expensive than the co-current configuration. The computation of fast permeating components requires further reduction of the relaxation factor and longer computational time. For example, a stiff system with two counter-current stages, a permeate recycle and four components gases required approximately 6 min to converge.

While performing test it was found that for a single module the computational effort decreased for decreasing stage cuts, i.e. systems with relatively small permeate flows were computed faster. As for multistage systems, it was observed that the computational time was largely influenced by recycle flows, more precisely, the systems with relatively large recycle flows converged slower. Summing up, the algorithm is able to calculate easy as well as difficult systems within reasonable time. The computational effort required

for the solution is largely influenced by a series of factors like boundary conditions and system configuration. The computational time can be minimised by the optimisation of the relaxation factor.

As far as the discretisation scheme is concerned, the computation of finite differences using the second order upwind scheme instead of the first order upwind scheme (Eqs. (9) and (10)) virtually did not improve the accuracy.

3. Experimental

3.1. Test rig

The feed gas was mixed using digital mass flow controllers 5850S provided by Brooks® Instrument (methane and carbon dioxide) and a digital mass flow controller red-y GSC provided by Vögtlin Instruments (oxygen). The permeate flow was measured using a digital mass flow meter 5860S provided by Brooks® Instrument. The heating oven Venticell 222R supplied by MMM-Group was used to provide isothermal conditions. The temperature of the feed gas was measured by a three-wire resistance thermometer purchased from JUMO. The absolute pressure values in the retentate and in the permeate channel were measured by electronic pressure transmitters PTX 1400 provided by GE Sensing. The retentate pressure was controlled by a proportional valve type 2834 provided by Bürkert. The retentate gas compositions were analysed using a mass spectrometer OmniStar provided by Balzers Instruments. The experiment control and data acquisition was performed by a PLC type RX3i provided by GE Fanuc. The tested membrane module consisted of 800 polyimide hollow fibres with the length of 0.38 m and the total membrane area of $0.38\,m^2$. To obtain pure gas permeances, the variable pressure tests were run for each of the gases. The pure gas permeances were calculated by determining the average from several measurements. Plasticisation was not observed during measurements for the range of pressures used (up to 10 bar). The determined pure gas permeances were: $\Pi_{CH_4} = 1.59e-6\,m^3_{STP}/(m^2\,bar)$, $\Pi_{CO_2} = 5.91e-5\,m^3_{STP}/(m^2\,bar)$ and $\Pi_{O_2} = 1.36e-5\,m^3_{STP}/(m^2\,bar)$. The relative error of the determined permeances equals $\pm 2\%$. The gas cylinders with the pure gases as well as the gas mixture for the calibration of the mass spectrometer were provided by Air Liquide. The flow diagram of the test rig is shown in Fig. 3. Due to technical reasons, only bore-side feed configurations were tested. However, the algorithm allows calculation of both bore-side feed and shell-side feed configurations.

3.2. Variable feed flow tests

A three-component biogas-like mixture was used for the model verification. Biogas is a multicomponent mixture that contains mainly methane and carbon dioxide with smaller amounts of other gases [31]. Recently, more focus has been put on the biogas upgrading due to environmental reasons and the membrane gas
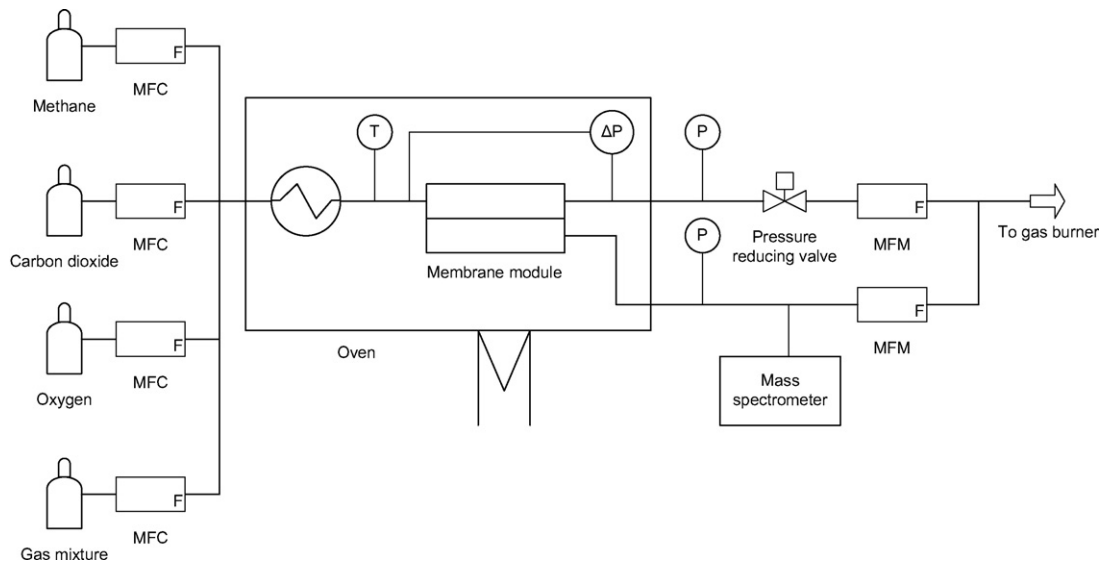
Fig. 3. Flowsheet of the experimental setup.

permeation proves to be a reasonable choice for this task [32,31,33]. Besides the model verification purposes, the permeation of a multi-component biogas-like mixture could be interesting for the design of gas permeation systems for biogas upgrading. Since the common objective for the biogas upgrading is the production of a natural gas substitute, the purified biogas must fulfil natural gas standards of the supplied natural gas grid. The natural gas standards usually limit the content of secondary components [31]. As a result, not only permeation of carbon dioxide and methane but also permeation of other components should be considered. In case of this experiment, the permeation of methane and carbon dioxide with an addition of oxygen was investigated.

The feed gas mixture consisted of the following gas volume fractions: $X_{CH_4} = 0.645$, $X_{CO_2} = 0.345$ and $X_{O_2} = 0.01$. The absolute pressures in the retentate and in the permeate were constant and equal to 9 bar and 1.1 bar respectively. The feed gas temperature equaled 43.3 °C. The total feed volume flow was varied within the limits of 1.5 l_{STP}/min and 5 l_{STP}/min. The modelling embraced a wider spectrum of feed volume flows: from 1 l_{STP}/min up to 15 l_{STP}/min. Both configurations: co-current and counter-current were tested.
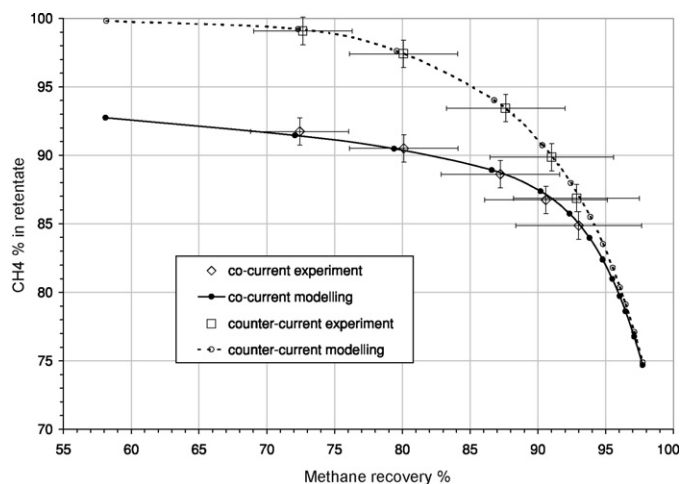
4. Results and discussion

Fig. 4 compares the performance of the tested module that was achieved during the experiment with the numerical model. The values predicted by the model fit well into the experimental data within the error limits. It can be noticed that for lower stage cuts the
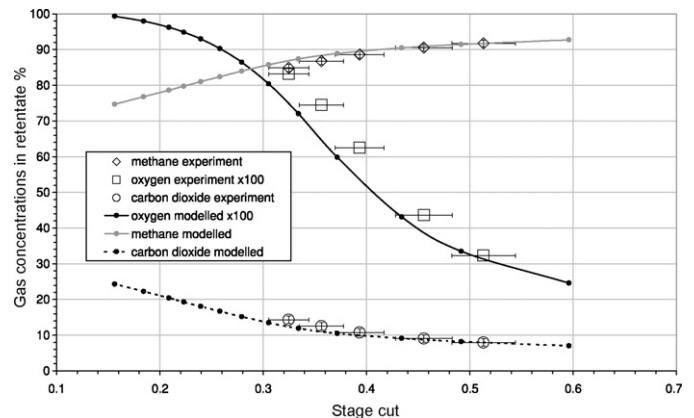

Fig. 5. Modelled and measured gas concentrations versus stage cut for the co-current flow.
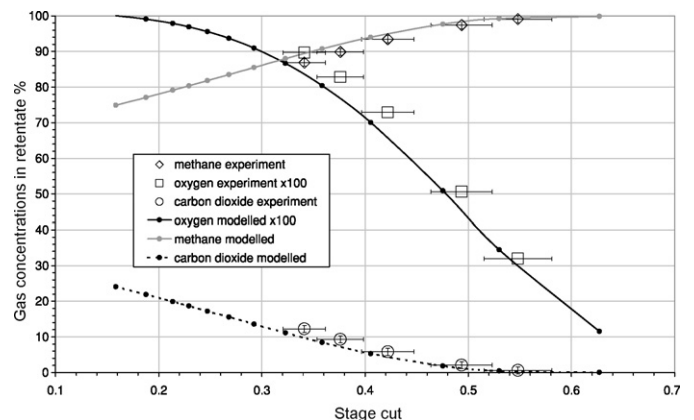

Fig. 4. Modelled and measured methane concentration versus methane recovery.

Fig. 6. Modelled and measured gas concentrations versus stage cut for the counter-current flow.
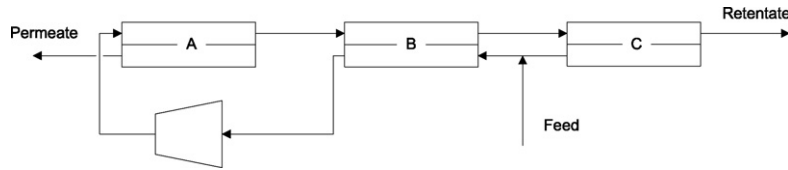
Fig. 7. Three-stage low-pressure feed cascade LP1-3a [30].

gas separation becomes similar for both configurations. This agrees with the assumptions of Pan [4] that the flow on the permeate side can be simplified for the calculation of 'high-flux' permeation. For higher stage cuts, both configurations provide visibly different results; the counter-current configuration is able to obtain higher methane concentrations in retentate than the co-current configuration.

The retentate gas concentrations for variable stage cuts are presented in Fig. 5 for the co-current configuration and in Fig. 6 for the counter-current configuration. The modelled values are in good agreement with the measured values. The model slightly overestimates methane enrichment, which can be attributed to the model simplifications and to the error in the measurement.

The absolute error of the concentration measurements was assumed to be 1%. Higher error limits of the methane recovery and the stage cut result from the error in measurement of the mixed gases volume flow.

As shown by the modelling and experiment, the single counter-current module is able to reach high methane concentrations and simultaneously reduce the fraction of oxygen in the produced retentate gas.

5. Conclusions

The presented algorithm is an iterative numerical method for the calculation of gas permeation systems equipped with hollow-fibre modules. The algorithm is able to calculate the permeation of multicomponent gas mixtures in co-current, counter-current and cross-flow configurations. The permeators can be arranged in any cascade with arbitrary number of recycles. The algorithm permits also the calculation of systems with additional nonlinearities like variable permeances or the feed pressure loss.

When performing computational test, large differences in the computational effort for various gas permeation configurations became apparent. While systems using the co-current flow configuration could be solved within a fraction of a second, the systems arranged in the counter-current required considerably much more time to converge. In addition, the computational effort was influenced by the stiffness of the system; the permeation of gases with relatively high selectivities required a reduction of the relaxation factor and longer computation.

The solution provided by the algorithm has been verified with experimental results for a single permeator in the co-current configuration and in the counter-current configuration for a three-component gas consisting of methane, carbon dioxide and oxygen. The results provided by the modelling agreed well with the experiment.

The future work connected with the algorithm could include an automatic adjustment of the relaxation factor to the stiffness of the problem, a concentration polarisation model, and optimisation methods.

Acknowledgements

Appendix A.

We consider a solution procedure for the calculation of the three-stage low-pressure feed cascade presented in Fig. 7. The solution of the system starts with the initialisation. Provided that the concentration of gas component i in the inlet to the mixer between cascades B and C is X_i, its initial concentrations in both feed channel and permeate channel of the stages A, B and C are given by:

$$x_{i,j}^A = X_i, \tag{A.1}$$

$$x_{i,j}^B = X_i, \tag{A.2}$$

$$x_{i,j}^C = X_i, \tag{A.3}$$

$$y_{i,j}^A = \frac{x_{i,j}^A \Pi_i}{\sum_{i=1}^{k} x_{i,j}^A \Pi_i}, \tag{A.4}$$

$$y_{i,j}^B = X_i, \tag{A.5}$$

$$y_{i,j}^C = \frac{x_{i,j}^C \Pi_i}{\sum_{i=1}^{k} x_{i,j}^C \Pi_i}. \tag{A.6}$$

The iteration begins with stage C. The volume flows of separate gas components are calculated with Eqs. (14) and (15) and subsequently with Eqs. (16) and (17). The calculation of volume flows for every discrete point is followed by the calculation of concentrations. The next step is the update of the boundary conditions for stage B followed by the same calculation procedure as for stage C:

$$F_{i,1}^B = F_{i,c}^A, \tag{A.7}$$

$$P_{i,1}^B = P_{i,c}^C + V X_i. \tag{A.8}$$

Finally, the boundary conditions for cascades A and C are updated, and the usual calculation procedure is executed:

$$F_{i,1}^A = P_{i,c}^B, \tag{A.9}$$

$$F_{i,1}^C = F_{i,c}^B. \tag{A.10}$$

After every iteration the convergence check for each of the discrete points is performed. Provided that the convergence criterion has reached the desired level the looping is interrupted.

Nomenclature

List of symbols

d	diameter of active layer (m)
D	internal diameter of fibre (m)
F	volume flow in feed (m_{STP}^3/s)
l	longitudinal coordinate (m)
p	pressure (bar)
P	volume flow in permeate (m_{STP}^3/s)
Q	trans-membrane flow (m^3/s)

s	total of fibres
T	temperature (K)
V	cascade inlet volume flow (m^3_{STP}/s)
x	gas volume fraction in feed
X	cascade inlet gas volume fraction
y	gas volume fraction in permeate
α	ideal selectivity
δ	convergence criterion (m^3_{STP}/s)
η	dynamic viscosity (kg/(m s))
Π	permeance ($m^3_{STP}/(m^2 s)$)
ϖ	relaxation factor

Superscripts

$'$	length specific
$''$	area specific
k	total of components
n	iteration index

Subscripts

i	component index
j	discrete point index
c	total of feed/permeate discrete points
F	referring to feed
P	referring to permeate
STP	standard temperature and pressure

References

[1] S.A. Stern, S.C. Wang, Countercurrent and cocurrent gas separation in a permeation stage. Comparison of computation methods, Journal of Membrane Science 4 (1978–1979) 141–148.
[2] S.A. Stern, J.E. Perrin, E.J. Naimon, Recycle and multimembrane permeators for gas separations, Journal of Membrane Science 20 (1) (1984) 25–43.
[3] F.P. McCandless, Iterative solution of multicomponent permeator model equations, Journal of Membrane Science 48 (1) (1990) 115–122.
[4] C.Y. Pan, Gas separation by high-flux, asymmetric hollow-fiber membrane, AIChE Journal 32 (12) (1986) 2020–2027.
[5] B.D. Bhide, S.A. Stern, A new evaluation of membrane processes for the oxygen-enrichment of air. I. Identification of optimum operating conditions and process configuration, Journal of Membrane Science 62 (1) (1991) 13–35.
[6] B.D. Bhide, S.A. Stern, Membrane processes for the removal of acid gases from natural gas. I. Process configurations and optimization of operating conditions, Journal of Membrane Science 81 (3) (1993) 209–237.
[7] S.P. Kaldis, G.C. Kapantaidakis, G.P. Sakellaropoulos, Simulation of multicomponent gas separation in a hollow fiber membrane by orthogonal collocation—hydrogen recovery from refinery gases, Journal of Membrane Science 173 (1) (2000) 61–71.
[8] M.H.M. Chowdhury, X. Feng, P. Douglas, E. Croiset, A new numerical approach for a detailed multicomponent gas separation membrane model and Aspenplus simulation, Chemical Engineering & Technology 28 (7) (2005) 773–782.
[9] S.-T. Hwang, J.M. Thorman, The continuous membrane column, AIChE Journal 26 (4) (1980) 558–566.
[10] K. Li, D.R. Acharya, R. Hughes, Mathematical modelling of multicomponent membrane permeators, Journal of Membrane Science 52 (2) (1990) 205–219.
[11] T. Tsuru, S.-T. Hwang, Permeators and continuous membrane columns with retentate recycle, Journal of Membrane Science 98 (1–2) (1995) 57–67.
[12] M.J. Thundyil, W.J. Koros, Mathematical modeling of gas separation permeators—for radial crossflow, countercurrent, and cocurrent hollow fiber membrane modules, Journal of Membrane Science 125 (2) (1997) 275–291.
[13] D.T. Coker, B.D. Freeman, G.K. Fleming, Modeling multicomponent gas separation using hollow-fiber membrane contactors, AIChE Journal 44 (6) (1998) 1289–1302.
[14] H. Chen, G. Jiang, R. Xu, An approximate solution for countercurrent gas permeation separating multicomponent mixtures, Journal of Membrane Science 95 (1) (1994) 11–19.
[15] T. Pettersen, K. Lien, Design studies of membrane permeator processes for gas separation, Gas Separation & Purification 9 (3) (1995) 151–169.
[16] H. Lababidi, G.A. Al-Enezi, H.M. Ettouney, Optimization of module configuration in membrane gas separation, Journal of Membrane Science 112 (2) (1996) 185–197.
[17] R. Qi, M.A. Henson, Membrane system design for multicomponent gas mixtures via mixed-integer nonlinear programming, Computers & Chemical Engineering 24 (12) (2000) 2719–2737.
[18] R.V. Uppaluri, R. Smith, P. Linke, A.C. Kokossis, On the simultaneous optimization of pressure and layout for gas permeation membrane systems, Journal of Membrane Science 280 (1–2) (2006) 832–848.
[19] H. Chang, W.-C. Hou, Optimization of membrane gas separation systems using genetic algorithm, Chemical Engineering Science 61 (16) (2006) 5355–5368.
[20] J.G. Wijmans, R.W. Baker, The solution-diffusion model: a review, Journal of Membrane Science 107 (1–2) (1995) 1–21.
[21] J. Anderson, Computational Fluid Dynamics, McGraw-Hill, 1995.
[22] B. Poling, J. Prausnitz, J. O'Connell, The Properties of Gases and Liquids, McGraw-Hill, 2000 (Chaps. 9-4 and 9-5).
[23] A. Mourgues, J. Sanchez, Theoretical analysis of concentration polarization in membrane modules for gas separation with feed inside the hollow-fibers, Journal of Membrane Science 252 (1–2) (2005) 133–144.
[24] S. Bhattacharya, S.-T. Hwang, Concentration polarization, separation factor, and Peclet number in membrane processes, Journal of Membrane Science 132 (1) (1997) 73–90.
[25] G. He, Y. Mi, P.L. Yue, G. Chen, Theoretical study on concentration polarization in gas separation membrane processes, Journal of Membrane Science 153 (2) (1999) 243–258.
[26] O. Lüdtke, R.D. Behling, K. Ohlrogge, Concentration polarization in gas permeation, Journal of Membrane Science 146 (2) (1998) 145–157.
[27] A.L. Zydney, Stagnant film model for concentration polarization in membrane systems, Journal of Membrane Science 130 (1–2) (1997) 275–281.
[28] R. Rautenbach, A. Struck, T. Melin, M.F.M. Roks, Impact of operating pressure on the permeance of hollow fiber gas separation membranes, Journal of Membrane Science 146 (2) (1998) 217–223.
[29] M.J. Thundyil, Y.H. Jois, W.J. Koros, Effect of permeate pressure on the mixed gas permeation of carbon dioxide and methane in a glassy polyimide, Journal of Membrane Science 152 (1) (1999) 29–40.
[30] J. Xu, R. Agrawal, Gas separation membrane cascades. I. One-compressor cascades with minimal exergy losses due to mixing, Journal of Membrane Science 112 (2) (1996) 115–128.
[31] M. Miltner, A. Makaruk, M. Harasek, Application of gas permeation for biogas upgrade—operational experiences of feeding biomethane into the Austrian gas grid, in: Proceedings of the 16th European Biomass Conference & Exhibition, Valencia, Spain, 2008, 2008, pp. 1905–1911.
[32] R. Rautenbach, Membranverfahren, Springer-Verlag, Berlin, 1997.
[33] M. Harasek, Are membrane based separation processes for the production of bio-methane and bio-hydrogen energy-efficient? in: Proceedings of the 16th European Biomass Conference & Exhibition, Valencia, Spain, 2008, 2008, pp. 1894–1897.